RSC Advances

ROYAL SOCIETY OF CHEMISTRY

www.rsc.org/advances

Journal Name

ARTICLE

Pd nanoparticles embedded in the outershell of mesoporous core-shell catalyst for phenol hydrogenation in pure water

Received 00th January 20xx,
Accepted 00th January 20xx

DOI: 10.1039/x0xx00000x

www.rsc.org/

Fengwei Zhang [a], Shuai Chen [b], Huan Li [a], Xian-Ming Zhang [a] and Hengquan Yang* [a,c]

A multi-component mesoporous core-shell structured nanocatalyst was prepared via encapsulation of a hydrophobic mesoporous carbon with an amino-functionalized mesoporous silica, followed by coordination of palladium precursors and then reduction with $NaBH_4$ reagent. The resulting Pd/MCN@MS-NH_2 catalyst could be well-dispersed in aqueous medium owing to its inherent hydrophilic properties of mesoporous silica shell. The experimental results indicated that the Pd/MCN@MS-NH_2 catalyst had high catalytic activity and selectivity for the hydrogenation of phenol to cyclohexanone under 1 atm of H_2 at 80 ^{o}C for 3 h in pure water (conversion >99% and selectivity 99%). Furthermore, the catalyst can be easily recovered and reused sixth times without significant loss of catalytic activity.

Introduction

In recent years, the porous carbon-based materials (PCMs) have received a wide range of applications in fields such as environmental remediation, [1] gas adsorption/separation, [2] energy storage/conversion [3] drug delivery, [4,5] and catalysis [6,7] because of their high chemical and mechanical stability, large specific surface area, excellent electrical conductivity and an adjustable pore structure. Generally, the PCMs can be prepared either through an organic-organic assembly soft template or nanocasting using solid silica as hard template method.[8,9] Recent discoveries have demonstrated that the introduction of heteroatoms (nitrogen or other functional groups) could significantly improve the catalytic activity and stability of the PCMs.[10-13] Such as Ferdi Schüth groups have successfully fabricated N-doped hollow carbon spheres by a simple and effective soft-templating method and then encapsulated the PtCo bimetallic nanoparticles inside their cavity for catalytic hydrogenolysis of 5-hydroxymethylfurfural (HMF) to 2,5-dimethylfuran (DMF) with 98% yield after 2 h. [14] Wang et al. have prepared polymeric mesoporous graphitic carbon nitride (mpg-C_3N_4) through thermally induced self-condensation of cyanamide using Ludox HS40 as a hard template and the mpg-C_3N_4 anchored palladium catalyst exhibited superior activity and selectivity in hydrogenation reaction.[15-18] Meanwhile, Liang et al. have also synthesized a metal-free, N-doped mesoporous carbon catalyst through the polymerization of o-phenylenediamine in the presence of silica colloid followed by the pyrolysis, etching and ammonia activation strategy, and the prepared catalyst showed higher catalytic activity for the ORR and full-cell (Zn-air) performance than other reported metal-free catalysts and the state of the art Pt/C catalyst.[19] Thus it can be seen that the N-doped and other heteroatoms-modified PCMs are powerful micro/nano-sized catalyst materials for a variety of chemical transformations.

It is well-known that the cyclohexanone was an industrially important intermediate for the production of nylon 6, nylon 66 and polyamide resins, [20] which was generally prepared from either the oxidation of cyclohexane or the hydrogenation of phenol. [21,22] The former route was always implemented under high temperature and high pressure conditions, and the generated by-products often complicated the separation and recovery process. [23] The recent phenol hydrogenation route can be divided into "one-step" and "two-step" processes, in which the "two-step" process generally involves hydrogenation of phenol to cyclohexanol followed by dehydrogenation to cyclohexanone. [24,25] In comparison, the "one-step" selective hydrogenation of phenol to cyclohexanone is identified as an atom economical and environmental benign strategy for producing cyclohexanone, aiming to replace the existing cyclohexane oxidation and two-step phenol hydrogenation process. [26-30] Despite all this, the development of a general and efficient heterogeneous catalyst for the "one-step" selective hydrogenation of phenol to cyclohexanone in pure water and mild reaction conditions is still one of the most significant challenges for chemists.

To further develop highly active, selective and stable heterogeneous catalysts, researchers have made considerable efforts to design and fabricate nanocomposites with core-shell structures due to their unique physicochemical properties and

[a] Institute of Crystalline Materials, Shanxi University, Taiyuan 030006, P. R. China
[b] Analytical Instrumentation Center, Institute of Coal Chemistry, Chinese Academy of Sciences, Taiyuan 030001, P. R. China
[c] School of Chemistry and Chemical Engineering, Shanxi University, Taiyuan 030006, P. R. China
E-mail: hqyang@sxu.edu.cn

spatial effect. For example, well-designed core-shell or yolk-shell structured nanocatalysts have been reported to have enhanced catalytic activity and selectivity for many organic transformations.[31-37] Our previous study also demonstrated that the hydrophobic core/hydrophilic shell structured Pd/MS-C_3@MS-NH_2 catalyst displayed excellent catalytic activity and selectivity for phenol in aqueous solution due to the high specific surface area, well-developed mesoporous porosity and hydrophobic inner core.[38] Based on this principle, herein we designed and synthesized a novel Pd-based core-shell structured multifunctional nanocatalyst, which was composed of hydrophobic mesoporous carbon core, hydrophilic mesoporous silica shell and highly dispersed Pd nanoparticles. To our knowledge, this is the first report on the encapsulation of mesoporous carbon nanospheres with amino-functionalized mesoporous silica to prepare hydrophobic core/hydrophilic shell structured multifunctional catalyst for the selective hydrogenation of phenol in pure water. To our credit, compared with hydrophobic mesoporous carbon (MCN) and hydrophilic mesoporous silica (MS-NH_2) supported Pd catalysts, the as-obtained Pd/MCN@MS-NH_2 catalyst presented superior catalytic performance for the selective aqueous hydrogenation of phenol.

Experimental Section

Materials Cetyltrimethylammonium bromide (CTAB, 99%) was purchased from Nanjing Robiot Co., Ltd. Palladium (II) acetate ($Pd(OAc)_2$, ≥97%), tetraethyl orthosilicate (TEOS, 98%), formaldehyde aqueous solution (37 wt%) and sodium hydroxide (NaOH) were purchased from Sinopharm Chemical Reagent Co., Ltd. (3-Aminopropyl)trimethoxysilane (APTMS), Pluronic F127 and sodium borohydride ($NaBH_4$, 98%) were obtained from Aladdin Chemical Reagent Co., Ltd. Phenol was provide by Tianjin Tianxin Fine Chemical Development Center. All other chemicals were of analytical grade and used as received without any further purification.

Preparation of hydrophobic mesoporous carbon nanospheres (MCN)

The MCN were synthesized according to a literature method and with a slight modification.[39] Typically, 0.8 g of phenol and 2.1 mL of formaldehyde solution (37 wt%) were dissolved in 15 mL of NaOH aqueous solution (0.1 M) under vigorous stirring and then heated to 70 °C for 0.5 h. After that, 1.28 g of Pluronic F127 dissolved in 15 mL of deionized water was slowly added to the above solution under stirring. The resultant mixture was stirred at 66 °C for 2 h. Subsequently, 50 mL of deionized water was added to the above solution, which continued to agitate for 18 h. After cooling to room temperature, 260 mL of deionized water was added to dilute the solution. The obtained homogeneous red solution was then transferred into a Teflon-lined stainless-steel autoclave and heated for 24 h at 130 °C. After reaction, the mixture was collected by vacuum filtration and washed several times with deionized water and ethanol, and vacuum dried at 50 °C for 12 h. Finally, the dry yellow powders were carbonized at 750 °C in Ar atmosphere for 3 h.

Encapsulation of mesoporous carbon nanospheres with amine-functionalized mesoporous silica (MCN@MS-NH_2)

The MCN@MS-NH_2 nanocomposites were synthesized through a modified Stöber method.[40] In a typical process, 200 mg of MCN nanospheres were fully dispersed in a solution containing 150 mL of ethanol, 100 mL of deionized water, 0.3 g of CTAB and 1.0 mL of concentrated ammonia under ultrasonic vibration. Subsequently, 0.22 mL of TEOS and 0.1 mL of APTMS were injected into the solution and continued to stir for 8 h. Finally, the surfactant was extracted by refluxing 1.0 g of as-synthesized materials in 120 mL of ethanol solution containing 1.5 mL of concentrated HCl for 12 h. The surfactant-free samples were denoted as MCN@MS-NH_2.

Preparation of Pd/MCN@MS-NH_2 nanocatalyst

Typically, 66 mg of $Pd(OAc)_2$ was dissolved in 10 mL of toluene to form a homogeneous orange solution. After that, 1.0 g of MCN@MS-NH_2 was added into the solution, and the mixture was stirred for 4 h at room temperature. Then, 50 mg of $NaBH_4$ was slowly added into the reaction mixture under violent agitation. The color of the mixture turned to gray immediately upon addition. After stirring for another 2 h, the dark solid was isolated by centrifugation, washed three times with ethanol and dried overnight under vacuum at 50 °C. The ICP-OES analysis result demonstrated that the loading amount of Pd onto the Pd/MCN@MS-NH_2 catalyst was 2.95 wt%.

General procedure for selective phenol hydrogenation in pure water

A 10 mL glass vial containing a magnetic stirrer bar was charged with a mixture of phenol (48 mg, 0.5 mmol), Pd/MCN@MS-NH_2 (80 mg, 5.0 mol% Pd) and 3 mL of deionized water. The vial was purged three times with H_2 and filled with 1 atm of H_2 balloon. The reaction was continued with stirring for 3 h at 80 °C, cooled to room temperature and was analyzed by Agilent 7890A gas chromatography after extracting with ethyl acetate two times and dried with anhydrous Na_2SO_4.

Catalyst recycling

After the catalytic run, the Pd/MCN@MS-NH_2 catalyst was separated by decantation of the centrifuged reaction mixture. Then the catalyst was washed with deionized water and ethyl acetate for three times, and dried in vacuum at 50 °C for 6 h. After that, a new batch of phenol was added for the next catalytic run.

Characterization

Transmission electron microscope (TEM) was carried out on a FEI Tecnai G2 F20S-Twin using an accelerating voltage of 200 kV. For sample preparation, the powders were dispersed in ethanol with the assistance of sonication, and one drop of the solution was dropped onto a micro grid. XRD measurements

were performed on a Rigaku Ultima IV diffractometer using Cu-Kα radiation as the X-ray source in the 2θ range of 10-80°. The N_2 adsorption-desorption isotherms were obtained on an ASAP2020 analyzer. Before measurement, samples were degassed under vacuum at 423 K for 6 h. Surface area of the samples was calculated by the Brunauer-Emmet-Teller (BET) method, and pore volume and pore size distribution were calculated using the Barrett-Joyner-Elmer (BJH) model. Thermogravimetric analysis (TGA) was determined on a SETARAM Evolution 16/18 apparatus. The samples were heated in an alumina pan from 25 °C to 800 °C at a heating rate of 10 °C/min under argon atmosphere. Fourier transform infrared (FTIR) spectra were obtained using a Nicolet NEXUS 670 spectrophotometer (frequency range from 4000 to 500 cm^{-1}) with KBr pellet. The X-ray photoelectron spectra (XPS) was analyzed on the PHI-5702 instrument and the C_{1s} line at 286.6 eV was used as the binding energy reference.

Results and Discussion

It is generally known that the mesoporous carbon nanospheres (MCN) possess excellent mechanical and thermal stability, in addition, they can concentrate the organic substrates around their surface through the π-π or hydrophobic interactions between the carbon moieties and phenyl rings of the substrates. Encouraged by these potential properties, thus the MCN are selected as building blocks for the core of core-shell structured nanocomposites. On the other hand, the amine-modified mesoporous silicas can not only effective stabilize the Pd NPs but also present excellent hydrophilicity owing to a plenty of Si-OH and -NH_2 groups on their inner channels. Therefore, it can be predicted that the combination of the hydrophobic carbon and hydrophilic silica motifs will have a far-reaching significance for practical applications. The synthetic procedure of hydrophobic carbon core/hydrophilic silica shell structured Pd/MCN@MS-NH_2 catalyst is illustrated in Scheme 1. Firstly, the MCN were synthesized via hydrothermal and carbonization treatment according to a reported protocol with slight modifications; Secondly, amino-functionalized mesoporous silica was uniformly coated onto the MCN surface by modified Stöber method and the CTAB template was removed by repeated extraction in ethanol solution containing concentrated HCl; Thirdly, the most of palladium precursors were immobilized by amino groups in the outer shell and a fraction of them were still penetrated into the internal core, and the target catalyst was obtained after reduction with $NaBH_4$.

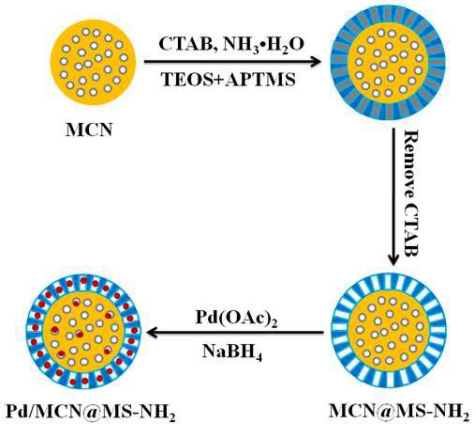

Scheme 1 The schematic diagram for the synthesis of Pd/MCN@MS-NH_2 catalyst.

The structure properties of as-prepared nanocomposites

The TEM images of the MCN and Pd/MCN@MS-NH_2 are shown in Fig. 1. It can be seen that the ordered cubic mesostructured MCN presented a uniform spherical morphology with a rough surface and an average diameter of about 210 nm, which was consistent with the literature reported results except the particle size.[9] As shown in Fig. 1c, the spherical shape and monodispersity of MCN had no obvious change, and only the particle size was increased significantly after encapsulation with hydrophilic mesoporous silica through a well-developed Stöber method, and the silica coating had the hexagonal P6mm mesostructure according to the Huang's result.[40] The TEM image of Pd/MCN@MS-NH_2 catalyst revealed that the silica shell thickness was about 20 nm and there were also many small Pd NPs embedded in the silica shells with an average diameter of 2.5 nm (Fig.S1 and Fig.S2a). The TEM images and size distribution of Pd/MCN and Pd/MS-NH_2 were presented in Fig. S3. Also the XPS results indicated the presence of C, Si, O, N and Pd species in the framework of the catalyst (Fig. 4a). It is worth mentioning that the mesoporous channels in the shell layer guaranteed the effective connection of the two kinds of ordered mesopores and also facilitated mass transport between the core and shell.

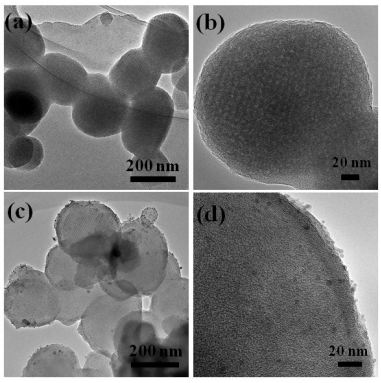

Fig. 1 The TEM images of (a) MCN, (b) enlarged MCN, (c) MCN@MS-NH_2 and (d) enlarged Pd/MCN@MS-NH_2.

The FT-IR spectra of the as-prepared MCN, MCN@MS-NH_2 and Pd/MCN@MS-NH_2 are shown in Fig. 2a. As can be seen from Fig. 2a, the MCN did not show any peaks because the graphitic carbon without infrared activity. In terms of MCN@MS-NH_2 and Pd/MCN@MS-NH_2, the absorption peak at 3442 cm^{-1} was assigned to the contribution of the -NH_2 group, which was overlapped by the -OH stretching vibrations of the Si-OH and physical adsorbed water. The peaks centered at 1076 cm^{-1} and 797 cm^{-1} corresponding to the Si-O asymmetric stretching and symmetric stretching vibrations. Additionally, the peaks appeared at 2928 cm^{-1}, 2859 cm^{-1}, 1630 cm^{-1} and 1382 cm^{-1} could be attributed to the stretching vibration of -CH_2, deformation vibration of O-H and bending vibration of C-H. The TGA curve of Pd/MCN@MS-NH_2 is exhibited in Fig. 2b. The thermogravimetric curve (TGA) can be divided into three stages: the first period of weight loss was about 2.9 wt% below 130 ^oC owing to the physical adsorbed water molecules, the second weight loss was about 15.3 wt% between 130 ^oC and 550 ^oC because of the decomposition of aminopropyl groups and the third segment can be attributed to the degradation of carbon core above 550 ^oC. The above results suggest that the MCN had successfully encapsulated with mesoporous silica shell and amino groups were also incorporated into the surface of MCN@MS-NH_2.

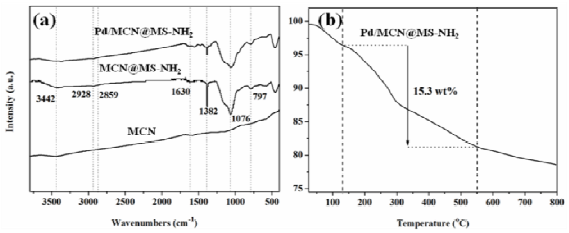

Fig. 2 (a) The FT-IR spectra of MCN, MCN@MS-NH_2, Pd/MCN@MS-NH_2 and (b) the TGA curve of Pd/MCN@MS-NH_2.

Fig. 3a showed the typical XRD pattern of the MCN, MCN@MS-NH_2 and Pd/MCN@MS-NH_2. In the case of MCN sample, the two broad diffraction peaks at 2θ = 20.5^o and 43.6^o can be indexed as the (002) and (100) reflections of graphitic carbon. For MCN@MS-NH_2, the broad diffraction peak at around 22.7^o was assigned to the amorphous silica. As for Pd/MCN@MS-NH_2, the XRD revealed that the existence of graphitic carbon, and one hardly observed the diffraction peak of metal Pd NPs. It is probably because that the very small Pd NPs, uniformly dispersion as well as low palladium loadings. The N_2 adsorption-desorption isotherms of both MCN and Pd/MCN@MS-NH_2 showed pseudo-type-I curve with H1 hysteresis loop at high relative pressure (Fig. 3b). This phenomenon usually have relationship with microporous and nanoporous structure, which is consistent with the results reported in literature [39, 40]. The BET specific surface area, pore volume and pore size of MCN was calculated to be 549.8 m^2/g, 0.89 cm^3/g and 3.3 nm, respectively. As compared to that of MCN, the specific surface area, pore volume and pore size of Pd/MCN@MS-NH_2 was determined to be 211.9 m^2/g, 0.41 cm^3/g and 3.1 nm, respectively. The reasons for the reduced surface area and pore volume were probably because of partial siliceous precursors permeating into the mesoporous carbon channels and majority of Pd NPs embedding on the internal pores of mesoporous silica shell. Nevertheless, the as-prepared catalyst probably still has high permeability and mass transfer rate for organic substrates involved in a catalytic reaction.

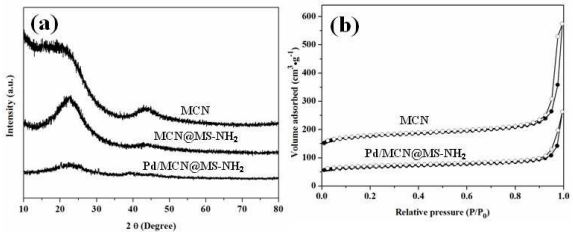

Fig. 3 (a) The XRD patterns of MCN, MCN@MS-NH_2 and Pd/MCN@MS-NH_2, (b) the N_2 adsorption-desorption isotherms of MCN and Pd/MCN@MS-NH_2.

To obtain further insight into the surface elemental composition and electron valence state of the Pd/MCN@MS-NH_2 catalyst, the catalyst was determined using X-ray photoelectron spectroscopy (XPS) technology. Fig. 4a displayed elemental survey scans of the surface composition of Pd/MCN@MS-NH_2 catalyst. Peaks corresponding to oxygen, carbon, nitrogen, silicon and palladium are clearly observed. The corresponding Pd 3d region is shown in Fig. 4b. It is observed that the XPS spectra of Pd 3d are composed of two asymmetric peaks ascribed to Pd $3d_{5/2}$ and Pd $3d_{3/2}$, which can be fitted using two doublets. The peaks around 335.1 and 340.6 eV are assigned to Pd (0), while those around 336.2 and 342.0 eV are corresponding to the Pd^{2+} species. What's more, the ratio of Pd (0) is as high as 60.3% and the ratio of the Pd^{2+} species is 39.7% in the Pd/MCN@MS-NH_2 catalyst.

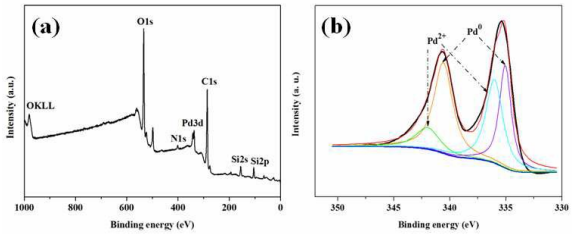

Fig. 4 The XPS spectra of (a) Pd/MCN@MS-NH_2 catalyst and (b) enlarged area of Pd_{3d}.

The selective hydrogenation of phenol over different catalysts

Table 1 Selective hydrogenation of phenol to cyclohexanone by various catalysts[a]

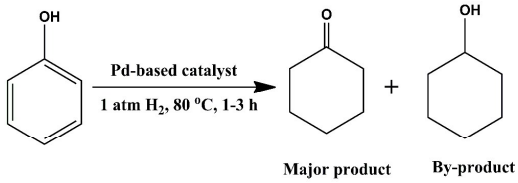

Entry	Catalyst	T (°C)	t (h)	Conv. (%) [b]	Sel. (%) [b]
1	MCN@MS-NH_2	80	3	0.7	>99
2	Pd/MCN	80	3	83.3	97.4
3	Pd/MS-NH_2	80	3	77.9	>99
4	Pd/MCN@MS-NH_2	80	1	42.8	>99
5	Pd/MCN@MS-NH_2	80	2	65.2	99
6	Pd/MCN@MS-NH_2	100	2	70.3	99
7	Pd/MCN@MS-NH_2	80	3	>99	99
8	Pd/MCN@MS-NH_2[c]	80	3	79.7	99
9	Pd/MCN@MS-NH_2[d]	80	3	20.4	99
10	Pd/MCN@MS-NH_2	60	3	49.5	99
11	Pd/MCN@MS-NH_2[e]	80	3	>99	99

[a] Reaction conditions: 0.5 mmol of phenol, 80 mg of catalyst (5.0 mol%) and 3.0 mL of H_2O under 1 atm of H_2. [b] The conversion and selectivity were determined by Agilent 7890A gas chromatograph. [c] 40 mg of catalyst (2.5 mol%). [d] 20 mg of catalyst (1.2 mol%). [e] 80 mg of catalyst (5.0 mol%) and 0.8 MPa of H_2.

The catalytic test results of palladium-based heterogeneous catalysts toward the selective hydrogenation of phenol to cyclohexanone under different reaction conditions are summarized in Table 1. It was observed that the conversion of phenol was only 0.7% and the selectivity of cyclohexanone was >99% in the presence of MCN@MS-NH_2 support at 80 °C for 3 h (Table 1, entry 1). When using Pd/MCN as a catalyst, a conversion of 83.3% and selectivity of 97.4% was obtained, and Pd/MS-NH_2 gave a lower conversion of 77.9% and a higher selectivity of >99%. Interestingly, in the case of Pd/MCN@MS-NH_2 catalyst, the conversion of phenol was >99% and the selectivity of cyclohexanone was 99% (Table 1, entry 7). The reasons for such high activity and selectivity can be attributed to the following factors: the mesoporous carbon nanospheres played a predominant role in the selective enrichment of phenol in pure water. In addition, the -NH_2 functionality in the silica framework can not only effectively stabilize the Pd NPs but also increase the concentration of phenol around the catalyst. When increasing the reaction temperature from 80 to 100 °C, the conversion of phenol was slightly increased from 65.2% to 70.3% and the selectivity of cyclohexanone still maintained at 99% for Pd/MCN@MS-NH_2 catalyst after reaction 2 h. As expected, increasing the palladium content from 1.2 mol% to 5.0 mol%, the conversion of phenol dramatically increased from 20.4% to >99%. However, when the reaction was carried out at 60 °C, the conversion of phenol decreased drastically to 49.5% and the selectivity of cyclohexanone still maintained at 99%. More interestingly, the selectivity of cyclohexanone still remained at 99% even if the reaction pressure increased to 0.8 MPa (Table 1, entry 11). The TON and TOF values of the Pd/MCN, Pd/MS-NH_2 and Pd/MCN@MS-NH_2 catalysts also presented in Table S1. The TOF value of Pd/MCN@MS-NH_2 catalyst was 1.22 and 1.27 times relative to Pd/MCN and Pd/MS-NH_2 catalyst, respectively. The aforementioned results suggested that the Pd/MCN@MS-NH_2 catalyst provided excellent catalytic activity and selectivity for the phenol hydrogenation in pure water.

The assessment of activation energy and recyclability

To explore the cause of excellent catalytic activity of Pd/MCN@MS-NH_2 catalyst, reaction kinetics of phenol hydrogenation in different temperatures were investigated. The reaction kinetics curves of phenol hydrogenation under the temperature from 50 to 70 °C are given in Fig. 5. As can be seen in Fig. 5, the conversion of phenol was increased gradually with the increase of the reaction time from 30-180 min. Furthermore, it was observed that when the reaction temperature increased from 50 to 70 °C, the conversion of phenol increased from 39.3% to 73.5%, whereas the selectivity of cyclohexanone still maintained nearly 100%. The results demonstrated that the yield of cyclohexanone constantly increased with reaction temperature increasing.

Fig. 6a displayed the plots of ln C_{phenol} versus reaction time under different temperatures. With the increasing of reaction temperature from 50 to 70 °C, the rate of phenol hydrogenation increased greatly over Pd/MCN@MS-NH_2 catalyst in pure water. It has been proved that the reaction kinetic of phenol hydrogenation was in accordance with pseudo-first order reaction kinetic model. Fig. 6b presented the Arrhenius plot of phenol hydrogenation under different reaction temperatures over Pd/MCN@MS-NH_2 catalyst. It was found that the apparent activation energy (Ea) of the Pd/MCN@MS-NH_2 catalyst was calculated to be 39.2 kJ·mol^{-1}, which showed a lower result compared to literature reported (48 kJ·mol^{-1}). [41] This apparently illustrated the synergistic effect between hydrophobic mesoporous carbon and hydrophilic mesoporous silica nanocomposites, which can significantly improve the mass transport and lower the activation energy barrier and enhance catalytic activity. The above results clearly indicated phenol hydrogenation was highly active and selective over the Pd/MCN@MS-NH_2 catalyst, which is, however, quite different from Pd/C generally producing a mixture of cyclohexanone and cyclohexanol with phenol conversion of 83.3% after 3 h.

Journal Name

ARTICLE

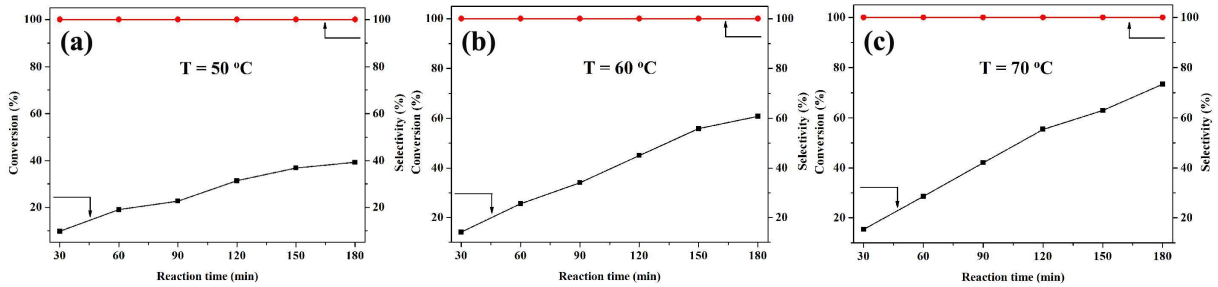

Fig. 5 The conversion and selectivity of phenol hydrogenation at different temperatures (a)50 °C, (b) 60 °C and (c) 70 °C over Pd/MCN@MS-NH_2 catalyst.

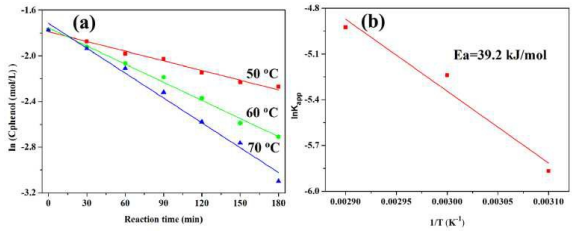

Fig. 6 (a) The plots of ln C_{phenol} versus reaction time and (b) the Arrhenius plot of phenol hydrogenation under over Pd/MCN@MS-NH_2 catalyst.

The stability and recyclability of the catalyst is a key factor for heterogeneous catalytic reaction. After the first run, the catalyst was separated from the aqueous medium through centrifugation, washed several times with ethyl acetate and dried under vacuum, and reused in subsequent runs under identical reaction conditions. As shown in Fig. 7, the catalyst exhibited significantly high catalytic activity for the phenol hydrogenation and the conversion maintained at 99% during the recycling, except that the conversion only slightly decreased to 96.4% in the fourth cycle. It is important to emphasize that the selectivity of cyclohexanone still reached up to 99% and almost no changes compared to fresh catalyst. The TEM image showed that the morphology of the recycled catalyst was almost not changed significantly, just the Pd NPs tended to be assemble into larger aggregates and the particle sizes increased from 2.5 nm to 4.5 nm (Supporting information, Fig. S2b). The recycled TEM images and leaching amount of Pd NPs of Pd/MCN and Pd/MS-NH_2 catalyst are shown in Fig. S4. The phenomenon confirmed that the tiny Pd NPs would be gathered together between each other during the phenol hydrogenation at 80 °C in pure water. After the recycling tests of the catalyst, the content of Pd was carried out through ICP-OES analysis. The result revealed that the amount of Pd was found to be about 2.93 wt%, suggesting that <0.8 wt% of Pd was leached from the catalyst surface. Furthermore, the hot filtration result revealed that the concentration of Pd NPs was only 0.073 mg/L in filtrate, suggesting the loss quantity was as low as 0.015%. As a result, the contribution of leached Pd NPs into the solution for the hydrogenation of phenol could be negligible. The ultrasonic washing of the catalyst during the recycling process also demonstrated that the leaching amount of Pd NPs was still at very low levels (total loss of six recycle <0.018 wt%, Table S2). Taking the aggregation of Pd NPs in the Pd/MCN@MS-NH_2 catalyst into account, the following work will be focused on preparing innovative multifunctional support to isolate and stabilize the Pd NPs through confined effect or coordination interaction, and simultaneously reducing the amount of Pd NPs and the temperature of phenol hydrogenation.

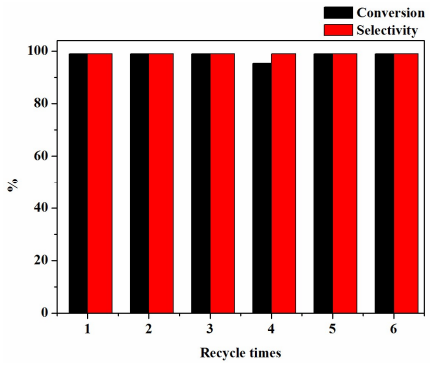

Fig. 7 Recycling tests of the Pd/MCN@MS-NH_2 catalyst in selective phenol hydrogenation. (Reaction conditions: 0.5 mmol of phenol, 3.0 mL of H_2O, 80 mg of catalyst, 1 atm of H_2, 80 °C, 3 h).

Conclusion

In summary, a simple and efficient methodology was proposed to prepare multifunctional core-shell structured Pd/MCN@MS-

NH_2 catalyst through direct encapsulation of a hydrophobic mesoporous carbon with a hydrophilic mesoporous silica, followed by adsorption-reduction of palladium metal precursors. The as-synthesized Pd/MCN@MS-NH_2 catalyst exhibited a superior catalytic activity and selectivity toward the selective hydrogenation of phenol under 1 atm of H_2 and 80 °C in pure water. Additionally, the reaction kinetics results showed that the catalyst possess a lower activation energy for the phenol hydrogenation compared to traditional heterogeneous catalysts. The reasons were probably due to the hydrogen bond interactions between phenol substrate and mesoporous silica as well as the π-π and hydrophobic enrichment effect of mesoporous carbon. More importantly, the catalyst displayed excellent recyclability and could be used for sixth times without significant loss of its catalytic activity. The future work will be devoted in particular to trying to decrease the reaction temperature of phenol hydrogenation and reduce the amount of noble metal catalyst.

Acknowledgements

This work was supported by the Scientific Research Start-up Funds of Shanxi University (023151801002), Natural Science Foundation for Young Scientists of Shanxi Province (2015021051) and Natural Science Foundation of China (20903064, 221173137).

References

1 L. Zhuang, Q. Li, J. Chen, B. Ma and S. Chen, *Chem. Eng. J.*, 2014, **253**, 24-33
2 A. Bhunia, I. Boldog, A. Möller and C. Janiak, *J. Mater. Chem. A.*, 2013, **1**, 14990-14999.
3 A. B. Fuertes and M. Sevilla, *ACS Appl. Mater. Interfaces*, 2015, **7**, 4344-4353.
4 P. Valle-Vigón, M. Sevilla and A. B. Fuertes, *Chem. Mater.*, 2010, **22**, 2526-2533.
5 H. Wan, H. Qin, Z. Xiong, W. Zhang and H. Zou, *Nanoscale*, 2013, **5**, 10936-10944.
6 Y. Yang, C. Sun, Y. Ren, S. Hao and D. Jiang, *Sci. Rep.*, 2014, **4**, 4540.
7 H. Mao, S. Peng, H. Yu, J. Chen, S. Zhao and F. Huo, *J. Mater. Chem. A.*, 2014, **2**, 5847-5851.
8 D.-S. Yang, C. Kim, M. Y. Song, H.-Y. Park, J. C. Kim, J.-J. Lee, M. J. Ju and J.-S. Yu, *J. Phys. Chem. C*, 2014, **118**, 16694-16702.
9 Y. Fang, D. Gu, Y. Zou, Z. Wu, F. Li, R. Che, Y. Deng, B. Tu and D. Zhao, *Angew. Chem. Int. Ed.*, 2010, **49**, 7987-7991.
10 P. Zhang, Y. Gong, H. Li, Z. Chen and Y. Wang, *Nat. Commun.*, 2013, **4**, 1593.
11 H. Chen, F. Sun, J. Wang, W. Li, W. Qiao, L. Ling and D. Long, *J. Phys. Chem. C*, 2013, **117**, 8318-8328.
12 J. Tang, J. Liu, C. Li, Y. Li, M. O. Tade, S. Dai and Y. Yamauchi, *Angew. Chem. Int. Ed.*, 2015, **54**, 588-593.
13 Z. Dong, C. Dong, Y. Liu, X. Le, Z. Jin and J. Ma, *Chem. Eng. J.*, 2015, **270**, 215-222.
14 G. H. Wang, J. Hilgert, F. H. Richter, F. Wang, H. J. Bongard, B. Spliethoff, C. Weidenthaler and F. Schüth, *Nat. Mater.*, 2014, **13**, 293-300.
15 Y. Wang, J. Yao, H. Li, D. Su and M. Antonietti, *J. Am. Chem. Soc.*, 2011,**133**, 2362-2365.
16 Y. Li, X. Xu, P. Zhang, Y. Gong, H. Li and Y. Wang, *RSC Adv.*, 2013, **3**, 10973-10982.
17 Y. Gong, P. Zhang, X. Xu, Y. Li, H. Li and Y. Wang, *J. Catal.*, 2013, **297**, 272-280.
18 X. Xu, M. Tang, M. Li, H. Li and Y. Wang, *ACS Catal.*, 2014, **4**, 3132-3135.
19 H. W. Liang, X. Zhuang, S. Brüller, X. Feng and K. Müllen, *Nat. Commun.*, 2014, **5**, 4973.
20 I. Dodgson, K. Griffen, G. Barberis, F. Pignataro and G. Tauszik, *Chem. Ind.*, 1989, 830-833.
21 Y. Wang, J. S. Zhang, X. C. Wang, M. Antonietti and H. R. Li, *Angew. Chem. Int. Ed.*, 2010, **49**, 3356-3359.
22 S. G. Shore, E. Ding, C. Park and M. A. Keane, *J. Mol. Catal. A: Chem.*, 2004, **212**, 291-300.
23 T. F. S. Silva, G. S. Mishra, M. F. Guedes da Silva, R. Wanke, L. Martins and A. J. L. Pombeiro, *Dalton Trans.*, 2009, 9207-9215.
24 M. Chatterjee, H. Kawanami, M. Sato, A. Chatterjee, T. Yokoyama and T. Suzuki, *Adv. Synth. Catal.*, 2009, **351**, 1912-1924.
25 V. Z. Fridman and A. A. Davydov, *J. Catal.*, 2000, **195**, 20-30.
26 H. Liu, T. Jiang, B. Han, S. Liang and Y. Zhou, *Science*, 2009, **326**, 1250-1252.
27 Z. Li, J. Liu, C. Xia and F. Li, *ACS Catal.*, 2013, **3**, 2440-2448.
28 C.-J. Lin, S.-H. Huang, N.-C. Lai and C.-M.Yang, *ACS Catal.*, 2015, Doi: 10.1021/acscatal.5b00380.
29 D. Zhang, Y. Guan, E. J. M. Hensen, T. Xue and Y. Wang, *Catal. Sci. Technol.*, 2014, **4**, 795-802.
30 D. Zhang, F. Ye, T. Xue, Y. Guan and Y. Wang, *Catal. Today*, 2014, **234**, 133-138.
31 Z.-A. Qiao, P. Zhang, S.-H. Chai, M. Chi, G. M. Veith, N. C. Gallego, M. Kidder and S. Dai, J. Am. Chem. Soc., 2014, 136, 11260-11263.
32 P. Zhang, Z.-A. Qiao and S. Dai, Chem. Commun., 2015, 51, 9246-9256.
33 H. Yang, X. Jiao and S. Li, *Chem. Commun.*, 2012, **48**, 11217-11219.
34 K. An, Q. Zhang, S. Alayoglu, N. Musselwhite, J.-Y. Shin and G. A. Somorjai, *Nano Lett.*, 2014, **14**, 4907-4912.
35 Q. Yue, Y. Zhang, C. Wang, X. Wang, Z. Sun, X.-F. Hou, D. Zhao and Y. Deng, *J. Mater. Chem. A*, 2015, **3**, 4586-4594.
36 D. Damodara, R. Arundhathi and P. R. Likhar, *Catal. Sci. Technol.*, 2013, **3**, 797-802.
37 X. Zhang, Y. Zhao, S. Xu, Y. Yang, J. Liu, Y. Wei and Q. Yang, *Nat. Commun.*, 2014, **5**, 3170.
38 F. Zhang and H. Yang, *Catal. Sci. Technol.*, 2015, **5**, 572-577.
39 Y. Fang, G. Zheng, J. Yang, H. Tang, Y. Zhang, B. Kong, Y. Lv, C. Xu, A. M. Asiri, J. Zi, F. Zhang and D. Zhao, *Angew. Chem. Int. Ed.*, 2014, **53**, 5366-5370.
40 Y. Wang, K. Wang, R. Zhang, X. Liu, X. Yan, J. Wang, E. Wagner and R. Huang, *ACS Nano*, 2014, **8**, 7870-7879.
41 C. Zhao, S. Kasakov, J. Y. He and J. A. Lercher, *J. Catal.*, 2012, **296**, 12-23.

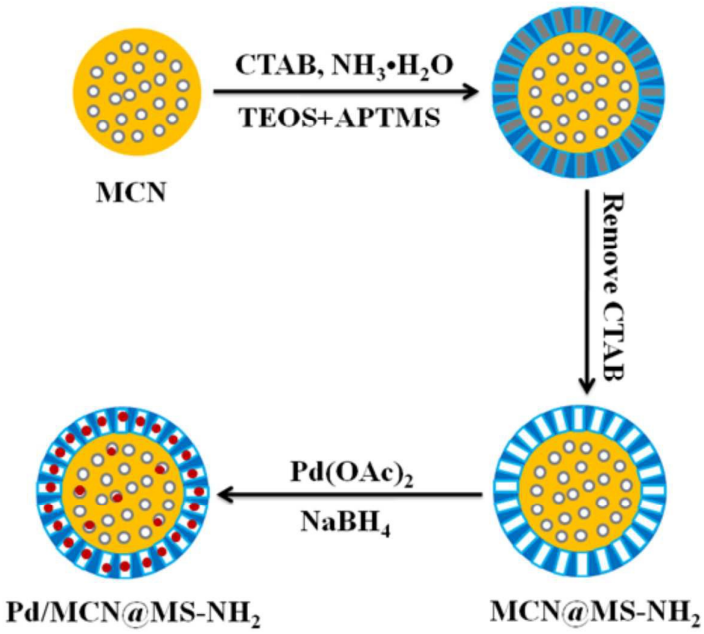

The Pd/MCN@MS-NH_2 catalyst simultaneously contains a hydrophobic carbon core and a hydrophilic silica shell, which is inclined to concentrate the phenol substrate around the active Pd NPs and exclude the cyclohexanone product off the catalyst surface.